IEEE Transactions on Systems, Man, and Cybernetics: Systems, Volume 53, Issue 12, December 2023, pp. 7583-7594
DOI:10.1109/TSMC.2023.3298217

Physics Informed Trajectory Inference of a Class of Nonlinear Systems using a Closed-Loop Output Error Technique

Adolfo Perrusquía, *Member, IEEE*, Weisi Guo, *Senior Member, IEEE*

***Abstract*—Trajectory inference is a hard problem when states measurements are noisy and if there is no high-fidelity model available for estimation; this may arise into high-variance and biased estimates results. This paper proposes a physics informed trajectory inference of a class of nonlinear systems. The approach combines the advantages of state and parameter estimation algorithms to infer the trajectory that follows the nonlinear system using online noisy state measurements. The algorithm is composed of a parallel estimated model constructed in terms of a low-pass filter parameterization. The estimated model defines a physics informed model that infers the trajectory of the real nonlinear system with noise attenuation capabilities. The parameters of the estimated model are updated by a closed-loop output error identification algorithm which uses the estimated states instead of the noisy measurements to avoid biased estimation. Stability and convergence of the proposed technique is assessed using Lyapunov stability theory. Simulations studies are carried out under different scenarios to verify the effectiveness of the proposed inference algorithm.**

***Index Terms*—Physics informed, inference, state parameterization, output error, nonlinear systems**

I. Introduction

In recent years, physics informed models (PIMs) [1] have become popular in several data driven algorithms for regression [2] and trajectory inference [3] of nonlinear systems. The key idea is to incorporate a high-fidelity model [4], [5] in the learning step as a guidance for parameters' updating, stabilization, and robustness. PIMs are also known as model-based algorithms [6] and can be used for other purposes such as: control policies design [7], gain tuning [8], and state observer models [9].

Physics informed neural networks (PINN) [1] are capable to incorporate the physics informed model as a regularization term to prevent large weights and fast convergence. However, normalized parameters are required to guarantee stable results of the PINN model which is a strong assumption for high dimensional systems with many parameters. This issue can be solved using series-parallel/parallel recurrent neural networks (RNN) [10], [11] which assume that the nonlinear system can be written as the sum of a multi-layer perceptron network and a stable linear dynamics. The main issue of this kind of networks is that weights convergence is not guaranteed and remain oscillating in bounded intervals and hence, this kind of RNN structures do not serve as a physics informed model. However, one of the main issues of any PIM is the assumption of parameters' knowledge. On the one hand, knowledge of the parameters ensures high accurate results in the regression/inference task. Conversely, biased parameters reduce the accuracy results and, in the worst case, may lead to instability of the complete network.

Kalman filter [12], [13] and its variants can be regarded as a kind of PIM which aim to infer the complete state of a given system using measurements of its output and an estimated model whose structure matches with the real system model under the same parameters and the Gaussian distributed noise assumption [14]–[16]. Despite this assumption provides robustness against modelling error [17], [18], a bad prior model could cause a fast divergence of the algorithm [19]. Novel techniques such has the EKFnet [20] combines neural networks capabilities and Kalman filter to estimate the best process and measurement noise covariance pair from the real measurement data. Nevertheless, this network may fit a large modelling error which produces a posterior estimation with high variance and hence, the accuracy of the estimated state will be poor.

In view of the above, it is mandatory to estimate the parameters of the nonlinear system to construct the PIM [21]. There exists an extensive literature for parameter identification [22], [23] based on least-squares (LS) and gradient-type rules and their variants [24]–[27]. The key idea to guarantee parameter estimates convergence is the fulfilment of a persistent of excitation (PE) condition [28]. However, if the measurements of the signals associated to the nonlinear system are noisy then biased estimates are obtained [29]. Therefore, there exists a trade-off between parameters and state estimation algorithms. Whilst state estimation algorithms require accurate parameters to infer the trajectory with high accuracy, the identification algorithm requires noise-free states measurements to avoid biased parameters estimates.

Some recent studies use closed-loop input (CLIE) [30], [31] and closed-loop output error (CLOE) techniques [32]–[34] for parameter estimation of robot manipulators [35], [36]. The idea behind these techniques is similar to the series-parallel/parallel RNN models where an estimated model of the real system is constructed; whose parameters are updated by an identification algorithm based on a LS or gradient rules of either the input error or output error of the estimated and real system. However, the CLOE algorithm requires well-tuned

This work was supported by the Royal Academy of Engineering and the Office of the Chief Science Adviser for National Security under the UK Intelligence Community Postdoctoral Research Fellowship programme.

A. Perrusquía and Weisi Guo are with the School of Aerospace, Transport and Manufacturing, Cranfield University, Bedford, UK
(e-mail: {Adolfo.Perrusquia-Guzman,Weisi.Guo}@cranfield.ac.uk).

filters to obtain smooth states measurements, otherwise biased estimates will be obtained [37]. Furthermore, the scope of the CLIE algorithm is limited to linear systems and for a small class of nonlinear Euler-Lagrange systems with constant inertia matrix [38].

Inspired by the above comments, this paper reports a physics informed algorithm that is able to infer the trajectory of an unknown nonlinear system using a closed-loop output error technique and online data. Here it is assumed that the nonlinear system is already controlled and cannot be modified; in addition, we only have access to states measurements. Nevertheless, some scenarios are considered where the control gain and desired trajectory/destination are available.

In contrast to classical state estimation algorithms that deals directly with the differential equation of the nonlinear system model, the proposed approach works with a state parameterization of the solution of the differential equation. This parameterization helps to construct a physics informed model that combines the advantages of state and parameter estimation algorithms to obtain an accurate trajectory inference. The contributions of this work with respect to previous developments for trajectory inference of nonlinear systems are the following:

- A novel physics informed model based on a new parameterization of the solution of the nonlinear system differential equation.
- Noise attenuation and parameter estimates convergence are simultaneously guaranteed under the fulfilment of a persistent of excitation (PE) condition.
- The algorithm can be easily extended for recurrent neural networks schemes which provides of robustness and stability in the weights' calculations.
- If we have access to the control input design, then the approach can be modified into an identification algorithm that can guarantee parameter estimates convergence to their real values under the fulfilment of a persistent of excitation (PE) condition.
- The proposed physics informed algorithm is supported by a rigorous stability proof, which proves that all the signals in the nonlinear closed-loop system are bounded under a non-zero approximation error.

The paper outline is as follows: Section II presents the problem formulation. Section III defines the state parameterization for the class of nonlinear systems used in this paper. Section IV presents the inference algorithm with trajectory incorporation. Section V gives some extensions of the proposed inference algorithm in recurrent neural networks and identification schemes. Section VI reports the simulation studies using a four dimensional F-16 aircraft dynamics. The conclusions are presented in Section VII.

Throughout this paper, $\mathbb{N}$, $\mathbb{R}$, $\mathbb{R}^+$, $\mathbb{R}^n$, $\mathbb{R}^{n\times m}$ denote the spaces of natural numbers, real numbers, positive real numbers, real n-vectors, and real $n\times m$-matrices, respectively; $I_n \in \mathbb{R}^{n\times n}$ denotes an identity matrix; $\lambda_{\min}(A)$ and $\lambda_{\max}(A)$ denotes the minimum and maximum eigenvalues of matrix A, respectively; $\otimes$ and $\text{vec}(A)$ defines the Kronecker product and the matrix stretch, the norms $\|A\| = \sqrt{\lambda_{\max}(A^\top A)}$ and $\|x\|$ stand for the induced matrix and vector Euclidean norms, respectively; where $x \in \mathbb{R}^n$, $A, B \in \mathbb{R}^{n\times n}$ and $n, m \in \mathbb{N}$.

II. Problem Formulation and Preliminaries

Consider the following continuous-time nonlinear system

$$\begin{aligned} \dot{x} &= f(x) + g(x)u, \quad x(t_0) = x_0, \\ z &= x + \omega, \quad \omega \sim \mathcal{N}(0, R), \end{aligned} \tag{1}$$

where $x \in \mathbb{R}^n$ denotes the state vector, $u \in \mathbb{R}^m$ is the control input, $z \in \mathbb{R}^n$ is a linear measurement model, $\omega \in \mathbb{R}^n$ defines noise drawn from a Gaussian distribution with mean zero and covariance $R = R^\top > 0 \in \mathbb{R}^{n\times n}$, $f(x) \in \mathbb{R}^n$ is the drift dynamics, and $g(x) \in \mathbb{R}^{n\times m}$ is the input dynamics. This kind of nonlinear systems are common in many mechanical, electrical, and hydraulic systems where the input u is linear with respect to $g(x)$ [39].

Assumption 1: Noisy state measurements are available from sensors. The control input structure and the desired trajectory can be known or unknown. These scenarios are discussed in future sections.

Assumption 2: The parameters of $f(x)$ and $g(x)$ are unknown. However, the structures of $f(x)$ and $g(x)$ are known.

Assumption 2 is used to parameterize linearly the nonlinear terms as a product of a matrix of basis functions $\phi(x)$ composed of known nonlinear terms and a vector θ of unknown parameters. For this purpose the next strong assumption is required

Assumption 3: The functions $f(x)$ and $g(x)$ are locally Lipschitz and can be approximated by a set of basis functions as it is stated in the Weierstrass higher-order approximation theorem [40].

Consider that we have a complete set of basis functions $\{\phi(x), \varphi(x)\}$ associated to the nonlinear system structure such that $f(x)$ and $g(x)$ can be exactly represented by

$$\begin{aligned} f(x) &= \phi^\top(x)\theta, \\ g(x)u &= \varphi^\top(x,u)\vartheta, \end{aligned} \tag{2}$$

where $\theta \in \mathbb{R}^{p_1}$ and $\vartheta \in \mathbb{R}^{p_2}$ are matrices composed of the unknown constant parameters; $\phi(x) : \mathbb{R}^n \to \mathbb{R}^{p_1\times n}$ and $\varphi(x,u) : \mathbb{R}^n \times \mathbb{R}^m \to \mathbb{R}^{p_2\times n}$ are basis functions of (1). Hence, the nonlinear system (1) can be equivalently written as

$$\dot{x} = \Phi^\top(x,u)\Theta, \tag{3}$$

where $\Theta = \begin{bmatrix}\theta \\ \vartheta\end{bmatrix} \in \mathbb{R}^p$, $\Phi(x,u) = \begin{bmatrix}\phi(x) \\ \varphi(x,u)\end{bmatrix} \in \mathbb{R}^{p\times n}$, $p = p_1 + p_2$.

Assumption 4: The control input $u \in \mathbb{R}^m$ stabilizes the nonlinear system (1) and ensures tracking of the desired reference $x^d \in \mathbb{R}^d$.

Consider an estimated model of (1) of the form

$$\begin{aligned} \dot{y} &= \widehat{f}(y) + \widehat{g}(y)v, \quad y(t_0) = x_0, \\ w &= y, \end{aligned} \tag{4}$$

where $y \in \mathbb{R}^n$ is the state of the estimated model, $v \in \mathbb{R}^m$ is the control input which has the same structure as the control input u, $w \in \mathbb{R}^n$ is the output of the reference model, $\widehat{f}(y) \in$

$\mathbb{R}^n$ and $\widehat{g}(y) \in \mathbb{R}^{n\times m}$ are approximations of f and g which satisfy the following parameterizations

$$\begin{aligned} \widehat{f}(y) &= \phi^\top(y)\widehat{\theta}, \\ \widehat{g}(y)v &= \varphi^\top(y,v)\widehat{\vartheta}, \end{aligned} \tag{5}$$

where $\widehat{\theta} \in \mathbb{R}^{p_1}$ and $\widehat{\vartheta} \in \mathbb{R}^{p_2}$ are the estimation matrices of θ and ϑ, respectively. The estimated model has two main objectives: 1) to construct a physics informed model that allows to infer the trajectory for a given input, and 2) attenuate noise from sensor measurements of the system states. Hence, the estimated model is written as

$$\dot{y} = \Phi^\top(y,v)\widehat{\Theta}, \tag{6}$$

where $\widehat{\Theta} = \begin{bmatrix} \widehat{\theta} \\ \widehat{\vartheta} \end{bmatrix} \in \mathbb{R}^p, \quad \Phi(y,v) = \begin{bmatrix} \phi(y) \\ \varphi(y,v) \end{bmatrix} \in \mathbb{R}^{p\times n}.$

Parameter estimates convergence is guaranteed if the vector of basis functions $\Phi(x,u)$ verifies the following persistent of excitation condition which is equivalent to the uniform complete observability (UCO) lemma [41].

Lemma 1: [42] The matrix $\Phi(x,u)$ is said to be persistent exciting in the time interval $[t : t+T]$ if there exists positive constants $\beta_0, \beta_1, T > 0$ such that the following holds for any time instance t

$$\beta_0 I \leq S_1 = \int_t^{t+T} \Phi(x,u)\Phi^\top(x,u)d\tau \leq \beta_1 I. \tag{7}$$

However, Assumption 1 establishes that we only have access to states measurements and knowledge of the control structure which may not necessarily fulfil the PE condition (7). To solve this issue an external excitation signal $\tau \in \mathbb{R}^n$ is added to the noisy states measurements, i.e.,

$$x_\tau := z + \tau, \tag{8}$$

such that the next PE condition (7) is satisfied. Without loss of generality x_τ is the output of the following nonlinear system

$$\dot{x}_\tau = f(x_\tau) + g(x_\tau)u_\tau, \tag{9}$$

where $u_\tau \in \mathbb{R}^m$ is the new control input which takes into account the excitation signal τ. The design of u_τ is discussed in future sections.

Define the output error between the nonlinear system states x_τ and the estimated model states y as

$$e := x_\tau - y. \tag{10}$$

Notice that if $y = x + \tau$, then the error is reduced to $e = \omega$ which means that only the noise measurement is preserved. This fact is equivalent to the innovation term in Kalman filter algorithms. The error dynamics between (9) and (4) is

$$\begin{aligned} \dot{e} &= \Phi^\top(x_\tau,u_\tau)\Theta - \Phi^\top(y,v)\widehat{\Theta} \\ &= (\Phi(x_\tau,u_\tau) - \Phi(y,v))^\top\Theta - \Phi^\top(y,v)\widetilde{\Theta}. \end{aligned} \tag{11}$$

Fig. 1 depicts the general block diagram of the proposed physics-informed algorithm. The algorithm is composed of two main elements: an estimated model (6) for trajectory estimation and an identification algorithm which updates the parameters of the estimated model using the output error (10). The main aim of the proposed approach is to estimate the parameters and trajectory of the nonlinear system such that both the parametric error $\widetilde{\Theta} = \widehat{\Theta} - \Theta$ and the identification error $e = x_\tau - y$ converge to zero.

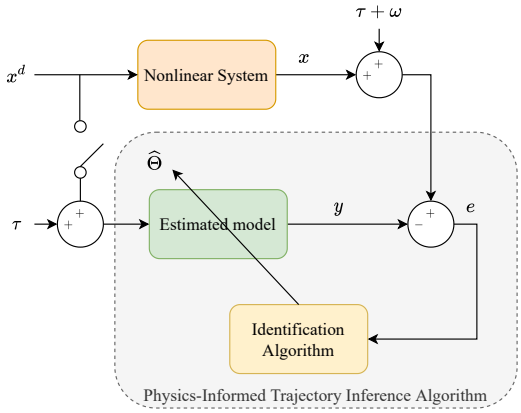

Fig. 1. Physics-Informed Trajectory Inference Algorithm block scheme

III. State Parameterization

Fig. 1 shows that the identification algorithm uses the output error e to estimate the parameters $\widehat{\Theta}$. However, the error dynamics (11) does not offer a direct way to relate the identification error e with the parametric error $\widetilde{\Theta}$. Furthermore, if the error dynamics (11) is used then the identification algorithm depends on $\dot{e}$ instead of e.

This section aims to develop a state parameterization which relates directly e with $\widetilde{\Theta}$. To achieve this goal and inspired in [43], [44], the nonlinear system (9) can be equivalently written as

$$\dot{x}_\tau = -\Lambda x_\tau + \Phi^\top(x_\tau,u_\tau)\Theta + \Lambda x_\tau, \tag{12}$$

where $\Lambda = \lambda I \in \mathbb{R}^{n\times n}$ and $\lambda > 0$. The additional term Λx_τ is used to obtain a linear system with input-to-state stability which is helpful to obtain a closed-form solution of the differential equation. The solution of (12) is

$$\begin{aligned} x_\tau(t) =& e^{-\Lambda(t-t_0)}x_\tau(t_0) + \int_{t_0}^t e^{\lambda(s-t)}\Phi^\top(x_\tau(s),u_\tau(s))ds\Theta \\ &+ \Lambda\int_{t_0}^t e^{\Lambda(s-t)}x_\tau(s)ds. \end{aligned}$$

Define

$$\begin{aligned} h(x_\tau) &:= \int_{t_0}^t e^{\lambda(s-t)}\Phi(x_\tau(s),u_\tau(s))ds \\ l(x_\tau) &:= \int_{t_0}^t e^{\Lambda(s-t)}x_\tau(s)ds. \end{aligned}$$

Then the solution of (1) is equivalently written as

$$x_\tau(t) = e^{-\Lambda(t-t_0)}x_\tau(t_0) + h^\top(x_\tau)\Theta + \Lambda l(x_\tau). \tag{13}$$

The terms $h(x_\tau)$ and $l(x_\tau)$ can be easily computed by the following low-pass filters

$$\begin{aligned} \dot{h}(x_\tau) &= -\lambda h(x_\tau) + \Phi(x_\tau,u_\tau), \quad h(x_\tau(t_0)) = 0, \\ \dot{l}(x_\tau) &= -\Lambda l(x_\tau) + x_\tau, \quad l(x_\tau(t_0)) = 0. \end{aligned} \tag{14}$$

Let $\Phi_\tau(x,u) = \Phi(x_\tau, u_\tau)$. Notice that

$$\begin{aligned}\|h(x_\tau)\| &\leq \int_{t_0}^{t} \left\| e^{\lambda(s-t)} \right\| \cdot \|\Phi_\tau(x,u)\| \, ds \\ &\leq \left(\int_{t_0}^{t} e^{2\lambda(s-t)} ds \right)^{\frac{1}{2}} \left(\int_{t_0}^{t} \Phi_\tau(x,u)\Phi_\tau^\top(x,u) ds \right)^{\frac{1}{2}}.\end{aligned}$$

The second integral can be written as a sum of $N = \frac{t-t_0}{T} - 1$ time-windows as

$$\int_{t_0}^{t} \Phi_\tau(x,u)\Phi_\tau^\top(x,u) ds = \sum_{\kappa=0}^{N} \int_{a}^{a+T} \Phi_\tau(x,u)\Phi_\tau^\top(x,u) ds,$$

where $a = t_0 + \kappa T$. Notice that the above integral is equivalent to N times the PE condition (7). So, the low-pass filter $h(x_\tau)$ is bounded by

$$\sqrt{\frac{\beta_0 N}{2\lambda}} \leq \|h(x_\tau)\| \leq \sqrt{\frac{\beta_1 N}{2\lambda}}. \tag{15}$$

The estimated model can also be written in terms of this new parameterization as

$$y(t) = e^{-\Lambda(t-t_0)} x_\tau(t_0) + h^\top(y)\widehat{\Theta} + \Lambda l(y) \tag{16}$$

Hence, the identification error verifies

$$\begin{aligned} e &= h^\top(x_\tau)\Theta - h^\top(y)\widehat{\Theta} + \Lambda[l(x_\tau) - l(y)] \\ &= -h^\top(y)\widetilde{\Theta} + \varepsilon, \end{aligned} \tag{17}$$

where $\varepsilon = [h(x_\tau) - h(y)]^\top \Theta + \Lambda[l(x_\tau) - l(y)]$ is a bounded approximation error, i.e., $0 \leq \|\varepsilon\| \leq \bar{\varepsilon}$, which decreases as $y \to x_\tau$ and $\bar{\varepsilon}$ is the upper bound of ε. Whilst the parameterization (11) requires to compute the time-derivative of the states x_τ, the parameterization (14) only needs measurements of the states and the output of the low-pass filters (14).

Theorem 1 establishes the uniform ultimate boundedness (UUB) [42] of the identification error e and boundedness of the parameter estimates $\widehat{\Theta}$ as long as the PE condition is fulfilled.

Theorem 1: Consider the identification error (17). Assume that the low-pass filter $h(y)$ in (14) is PE. If the parameter estimates $\widehat{\Theta}$ are updated as

$$\dot{\widehat{\Theta}} = \dot{\widehat{\Theta}} = \Gamma h(y) e \tag{18}$$

where $\Gamma \in \mathbb{R}^{p\times p}$ is a positive definite gain matrix, then the following statements are verified

1) The identification error e is UUB with a practical bound given by $\epsilon = (\frac{\beta_1}{\beta_0} + 1)\bar{\varepsilon}$.
2) The parametric error $\widetilde{\Theta}$ is UUB with a practical bound given by $\mu = \frac{2\lambda}{\beta_0 N}\sqrt{\frac{\beta_1 N}{2\lambda}}\bar{\varepsilon}$, and hence $\widehat{\Theta}$ remain bounded.

Proof: Consider the next Lyapunov function

$$V = \frac{1}{2}\text{tr}\{\widetilde{\Theta}^\top \Gamma^{-1} \widetilde{\Theta}\}. \tag{19}$$

The time-derivative of (19) along the system trajectories (18) is

$$\begin{aligned}\dot{V} &= \text{tr}\{\widetilde{\Theta}^\top \Gamma^{-1} \dot{\widetilde{\Theta}}\} \\ &= -\text{tr}\{\widetilde{\Theta}^\top h(y) h^\top(y) \widetilde{\Theta} - \widetilde{\Theta}^\top h(y)\varepsilon\} \\ &\leq -\lambda_{\min}^2(h(y))\|\widetilde{\Theta}\|^2 + \lambda_{\max}(h(y))\|\varepsilon\|\|\widetilde{\Theta}\|\end{aligned}$$

$\dot{V}$ is negative definite if

$$\begin{aligned}\|\widetilde{\Theta}\| &> \frac{\lambda_{\max}(h(y))}{\lambda_{\min}^2(h(y))}\|\varepsilon\| \\ \|\widetilde{\Theta}\| &> \frac{2\lambda}{\beta_0 N}\sqrt{\frac{\beta_1 N}{2\lambda}}\bar{\varepsilon} \equiv \mu.\end{aligned} \tag{20}$$

The bound (20) connects the convergence-time with the parametric error $\widetilde{\Theta}$. On the one hand, large number of time-windows N under the PE excitation condition fulfilment (7) ensures the parametric error $\widetilde{\Theta}$ converges to a bounded set S_μ of radius μ, i.e., $\|\widetilde{\Theta}\| \leq \mu$ and hence the trajectories are UUB.

From the identification error (17) we have that

$$\begin{aligned}\|e\| &\leq \|\widetilde{\Theta}\|\|h(y)\| + \|\varepsilon\| \\ &\leq \left(\frac{\beta_1}{\beta_0} + 1\right)\bar{\varepsilon}\end{aligned} \tag{21}$$

The above result is consistent to the proposed parameterization since the identification error e is directly related to the error of the low-pass filters $h(\cdot)$ and $l(\cdot)$. In addition, the term $\frac{\beta_1}{\beta_0}$ gives the highest upper bound of the identification error e. The smallest upper bound is given by $\|e\| \leq 2\bar{\varepsilon}$ since $\beta_0 \leq \beta_1$. This completes the first part of the proof.

The update rule (18) can be expressed as

$$\text{vec}(\dot{\widetilde{\Theta}}) = (I_n \otimes \Gamma h(y))e. \tag{22}$$

By using this notation, it is possible to express the update rule (18) as the following linear time-variant (LTV) system

$$\begin{aligned}\dot{\xi}(t) &= B(t)u(t) \\ \zeta(t) &= C(t)\xi(t),\end{aligned} \tag{23}$$

where $B(t) = I_n \otimes \Gamma h(y) \in \mathbb{R}^{np\times n}$, $C(t) = I_n \otimes h^\top(y) \in \mathbb{R}^{n\times np}$, $\xi(t) = \text{vec}(\widetilde{\Theta}) \in \mathbb{R}^{np}$, and $\zeta(t) = e(t) - \varepsilon(t)$. The above LTV model matches with the update rule (18) under the output feedback $u(t) = \zeta(t) + \varepsilon(t)$. Since ζ, e, and $h(y)$ are bounded and $h(y)$ is PE, then by the uniform complete observability (UCO) lemma [41] we can conclude that boundedness of e and ζ ensures boundedness of the parametric error $\widetilde{\Theta}$ and consequently $\widehat{\Theta}$ is also bounded.

The time-derivative of (19) can be written as

$$\begin{aligned}\dot{V} &\leq -\lambda_{\min}^2(h(y))\|\widetilde{\Theta}\|^2 + \lambda_{\max}(h(y))\|\varepsilon\|\|\widetilde{\Theta}\| \\ &\leq -\frac{\lambda_{\min}(\Gamma)\beta_0 N}{\lambda} V + \sqrt{\frac{\lambda_{\max}(\Gamma)\beta_1 N}{\lambda}} V\bar{\varepsilon} \\ &= -\alpha V + \beta V^{1/2}\end{aligned}$$

where $\alpha = \frac{\lambda_{\min}(\Gamma)\beta_0 N}{\lambda}$ and $\beta = \sqrt{\frac{\lambda_{\max}(\Gamma)\beta_1 N}{\lambda}}\bar{\varepsilon}$. Notice that the equation is in fact a Bernoulli differential equation which has the following solution

$$V(t) = \left(\frac{\beta}{\alpha} + \left(\sqrt{V(t_0)} - \frac{\beta}{\alpha}\right) e^{-\frac{1}{2}\alpha(t-t_0)}\right)^2. \tag{24}$$

The above result is consistent with the result of the first part of the proof. On the one hand, if the approximation error ε is large, then the convergence time will be fast because the radius μ of the set S_μ is large. On the other hand, for small approximation error ε the algorithm requires more time to converge into the bounded set S_μ. Furthermore, convergence

depends in the richness of the PE signal. Notice that if $\varepsilon \equiv 0$, then an exponential stable solution is obtained with a decay factor of α. This completes the second part of the proof. ■

From the results of Theorem 1 it follows that the error dynamics in (11) is also bounded because the regressor matrix Φ is bounded by construction and the parametric error $\widetilde{\Theta}$ is bounded, and hence, $\dot{e}$ is also bounded. Furthermore, since e is bounded and x_τ is bounded, then it follows that the state measurement y is also bounded.

Notice that the update rule (18) uses the estimated states y instead of the noisy measurements x_τ to construct the set of basis functions $h(y)$. This implies that the parameter estimates are not biased. In addition, the PE signal τ is also considered as a probing noise which attenuates the effect of the noise ω. The estimated trajectory $\widehat{x} \in \mathbb{R}^n$ can be easily extracted by subtracting the PE signal τ of the estimated model states y, that is,

$$\widehat{x} = y - \tau. \tag{25}$$

The previous formulation uses a complete set of basis functions such that the nonlinear functions $f(x_\tau)$ and $g(x_\tau)$ are well-defined. However, as it is stated in the Weierstrass higher-order approximation theorem, it is possible to find a complete independent basis set $\{\phi(x_\tau), \varphi(x_\tau)\}$ such that the nonlinear functions can be uniformly approximated by

$$\begin{aligned} f(x_\tau) &= \phi^\top(x_\tau)\theta + \varepsilon_f \\ g(x_\tau)u_\tau &= \varphi^\top(x_\tau, u_\tau)\vartheta + \varepsilon_g, \end{aligned} \tag{26}$$

where $\varepsilon_f \in \mathbb{R}^n$ and $\varepsilon_g \in \mathbb{R}^n$ define approximation errors which are assumed to be bounded, i.e., $0 < \|\varepsilon_f\| \leq \bar{\varepsilon}_f$ and $0 < \|\varepsilon_g\| \leq \bar{\varepsilon}_g$. Therefore, the approximation error is modified to $\varepsilon = \varepsilon_f + \varepsilon_g u_\tau + [h(x_\tau) - h(y)]^\top\Theta - \Lambda[l(x_\tau) - l(y)]$. The results of Theorem 1 hold for this case.

IV. Trajectory Incorporation

The previous section addresses the general form of the proposed trajectory inference algorithm. However, the desired trajectory/destination is hidden within the control input. Both the control input and the trajectory x^d can be either known or unknown which can benefit the algorithm with more information. Therefore, in this section three cases for trajectory incorporation are considered: i) known control gain and trajectory, ii) unknown control gain and known trajectory, and iii) unknown control gain and trajectory.

A. Known control gain and trajectory

For sake of simplicity, assume that the control input of (9) and (4) have the following linear structure

$$\begin{aligned} u_\tau &= -K(x_\tau - x^d - \tau - \omega), \\ v &= -K(y - x^d - \tau). \end{aligned} \tag{27}$$

where $K \in \mathbb{R}^{m\times n}$ is a stabilizing control gain and $x^d \in \mathbb{R}^n$ is a desired trajectory.

Remark 1: The control input u_τ can be designed with different structures and not necessarily a linear form. In general, controllers of the form $u_\tau = -Kw(x_\tau, x^d, \tau, \omega)$ can be used in this approach, where $w(\widetilde{x}) = w(x_\tau, x^d, \tau, \omega)$ is an error dependent function and K is the control gain.

Fig. 2 depicts the proposed inference algorithm for known control gain and trajectory. For this case, the control input v of the estimated model is used for the design of the basis functions vector $\Phi(y, v)$. It is important to highlight that knowledge of the control gain and destination helps to constraint the possible solutions of the inference algorithm to ensure bounded parameter estimates convergence.

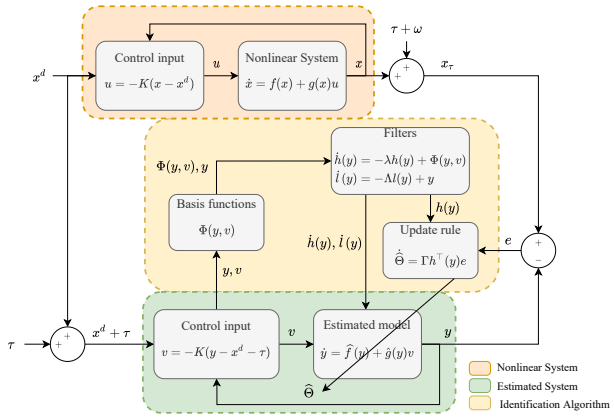

Fig. 2. Physics-Informed Trajectory Inference Algorithm block scheme for known control gain and trajectory

B. Unknown control gain and known trajectory

If the control gain K is unknown, then the control input v cannot be constructed. Nevertheless, it is possible to avoid v and use the desired trajectory x^d as input. The nonlinear dynamics (9) under the control input (27) yields the following nonlinear system

$$\begin{aligned} \dot{x}_\tau &= f(x_\tau) - g(x_\tau)Kx_\tau + g(x_\tau)K(x^d + \tau + \omega) \\ &= F(x_\tau) + G(x_\tau)(x^d + \tau + \omega), \end{aligned} \tag{28}$$

where $F(x_\tau) = f(x_\tau) - g(x_\tau)Kx_\tau \in \mathbb{R}^n$ and $G(x_\tau) = g(x_\tau)K \in \mathbb{R}^{n\times n}$. Both $F(x_\tau)$ and $G(x_\tau)$ are locally Lipschitz and can be linearly parametrized as

$$\begin{aligned} F(x_\tau) &= \psi_F^\top(x_\tau)\rho, \\ G(x_\tau)(x^d + \tau + \omega) &= \psi_G^\top(x_\tau, x^d + \tau + \omega)\varrho \end{aligned} \tag{29}$$

where $\rho \in \mathbb{R}^{p_3}$ and $\varrho \in \mathbb{R}^{p_4}$ are the new parameters, $\psi_F(x_\tau) : \mathbb{R}^n \to \mathbb{R}^{p_3\times n}$ and $\psi_G(x_\tau, x^d + \tau + \omega) : \mathbb{R}^n \times \mathbb{R}^n \to \mathbb{R}^{p_4\times n}$ are matrices of basis functions. Define $\Xi = [\rho^\top, \varrho^\top]^\top \in \mathbb{R}^{p_\xi}$ as the new vector of parameters and $\Psi(x_\tau, x^d + \tau + \omega) = \begin{bmatrix} \psi_F(x_\tau) \\ \psi_G(x_\tau, x^d + \tau + \omega) \end{bmatrix} \in \mathbb{R}^{p_\xi\times n}$ the new vector of basis functions, where $p_\xi = p_3 + p_4$. It follows that

$$\dot{x}_\tau = \Psi^\top(x_\tau, x^d + \tau + \omega)\Xi. \tag{30}$$

The new estimated model is

$$\dot{y} = \widehat{F}(y) + \widehat{G}(y)(x^d + \tau) = \Psi^\top(y, x^d + \tau)\widehat{\Xi}. \tag{31}$$

where $\widehat{\Xi} \in \mathbb{R}^{p_\xi}$ are estimates of Ξ. The state parameterizations of (30) and (31) are given by

$$\begin{aligned} x_\tau(t) &= e^{-\Lambda(t-t_0)}x_\tau(t_0) + H^\top(x_\tau)\Xi + \Lambda l(x_\tau) \\ y(t) &= e^{-\Lambda(t-t_0)}x_\tau(t_0) + H^\top(y)\widehat{\Xi} + \Lambda l(y) \end{aligned} \tag{32}$$

where $H(x_\tau), H(y) \in \mathbb{R}^{p_\xi \times n}$ are computed with the following low-pass filters

$$\begin{aligned} \dot{H}(x_\tau) &= -\lambda H(x_\tau) + \Psi(x_\tau, x^d + \tau + \omega), \\ \dot{H}(y) &= -\lambda H(y) + \Psi(y, x^d + \tau), \quad H(y(t_0)) = 0. \end{aligned} \tag{33}$$

The identification error between the state parameterizations (32) is given by

$$\begin{aligned} e &= H^\top(x_\tau)\Xi - H^\top(y)\widehat{\Xi} + \Lambda[l(x_\tau) - l(y)] \\ &= -H^\top(y)\widetilde{\Xi} + \varepsilon_H, \end{aligned} \tag{34}$$

where $\widetilde{\Xi} = \widehat{\Xi} - \Xi \in \mathbb{R}^{p_\xi}$ defines the parametric error and $\varepsilon_H = [H(x_\tau) - H(y)]^\top \Xi + \Lambda[l(x_\tau) - l(y)] \in \mathbb{R}^n$ is a bounded approximation error, i.e., $0 < \|\varepsilon_H\| \leq \bar{\varepsilon}_H$.

Fig. 3 depicts the proposed inference algorithm under the imposed constraints. Notice that the estimated model uses the desired reference with excitation as input to construct the basis function vector $\Psi(y, x^d + \tau)$. The other blocks of the diagram remain the same as the previous diagram in Fig. 2.

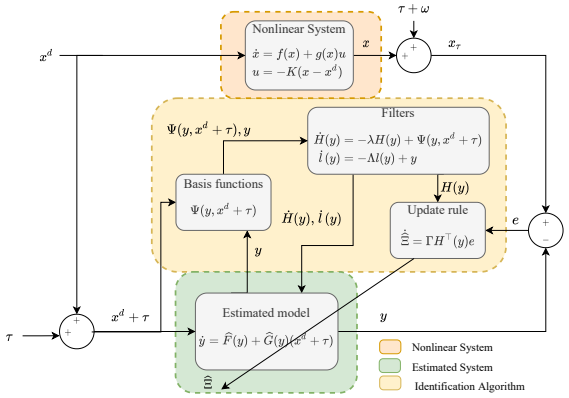

Fig. 3. Physics-Informed Trajectory Inference Algorithm block scheme for unknown control gain and known trajectory

C. Unknown control gain and trajectory

For this case both the control gain K and desired trajectory x^d are unknown, so we cannot use the previous parameterization for the inference algorithm design. To deal with this issue, consider the following new parameterization of (28)

$$F_x(x_\tau) = F(x_\tau) + G(x_\tau)x^d = \psi_H^\top(x)\sigma, \tag{35}$$

where $\sigma \in \mathbb{R}^{p_5}$ is a matrix of parameters and $\psi_H(x) : \mathbb{R}^n \to \mathbb{R}^{p_5 \times n}$ is a vector of basis functions. In this new parametrization the destination is within the parameters σ.

Remark 2: The desired trajectory/destination must be constant to guarantee parameter convergence. Otherwise, time-varying parameters will be obtained which prevents the inference algorithm to construct the physics informed model.

Then the nonlinear system is simplified to

$$\dot{x}_\tau = F_x(x_\tau) + G(x_\tau)(\tau + \omega). \tag{36}$$

Notice that only the excitation signal τ and the noise ω are used as input of the nonlinear system (36). The nonlinear system (36) is rewritten as

$$\dot{x}_\tau = \Omega^\top(x_\tau, \tau + \omega)\Sigma, \tag{37}$$

where $\Sigma = \begin{bmatrix} \sigma \\ \varrho \end{bmatrix} \in \mathbb{R}^{p_\sigma}$, $\Omega = \begin{bmatrix} \psi_H(x_\tau) \\ \psi_G(x_\tau)(\tau + \omega) \end{bmatrix} \in \mathbb{R}^{p_\sigma \times n}$ are the parameters and basis functions associated to unknown gain and trajectory scenario; with $p_\sigma = p_4 + p_5$. The estimated model under the new parameterization (37) is

$$\dot{y} = \Omega^\top(y, \tau)\widehat{\Sigma}, \tag{38}$$

where $\widehat{\Sigma} \in \mathbb{R}^{p_\sigma}$ is the vector of parameter estimates of Σ. The state-parameterization of both (37) and (38) are

$$\begin{aligned} x_\tau(t) &= e^{-\lambda(t-t_0)}x_\tau(t_0) + T^\top(x_\tau)\Sigma + \Lambda l(x_\tau), \\ y(t) &= e^{-\lambda(t-t_0)}x_\tau(t_0) + T^\top(y)\widehat{\Sigma} + \Lambda l(y). \end{aligned} \tag{39}$$

where $T(x_\tau)$ and $T(y)$ are computed by the following low-pass filters

$$\begin{aligned} \dot{T}(x_\tau) &= -\lambda T(x_\tau) + \Omega(x_\tau, \tau + \omega), \\ \dot{T}(y) &= -\lambda T(y) + \Omega(y, \tau), \quad T(y(t_0)) = 0. \end{aligned} \tag{40}$$

The identification error between (39) satisfies the following equation

$$\begin{aligned} e &= T^\top(x_\tau)\Sigma - T^\top(y)\widehat{\Sigma} + \Lambda[l(x_\tau) - l(y)] \\ &= -T^\top(y)\widetilde{\Sigma} + \varepsilon_T, \end{aligned} \tag{41}$$

where $\widetilde{\Sigma} = \widehat{\Sigma} - \Sigma \in \mathbb{R}^{p_\sigma}$ is the parametric error vector and $\varepsilon_T = [T(x_\tau) - T(y)]^\top \Sigma + \Lambda[l(x_\tau) - l(y)] \in \mathbb{R}^n$ is an approximation error.

Fig. 4 depicts the inference algorithm diagram. In this diagram only measurements of the noisy states of the nonlinear system are available. Here the basis functions use the excitation signal τ and the states of the estimated model y to construct the identification algorithm.

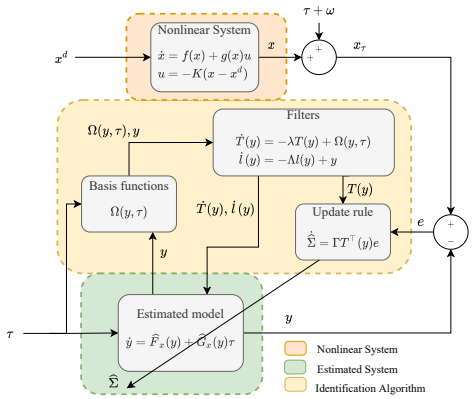

Fig. 4. Physics-Informed Trajectory Inference Algorithm block scheme for unknown control gain and trajectory

Theorem 1 holds for either the identification error (34) or (41), where the parameter estimates $\widehat{\Xi}$ or $\widehat{\Sigma}$ are updated instead of $\widehat{\Theta}$. In both cases, the vector of basis functions $\Psi(x_\tau, x^d + \tau)$ and $\Omega(x_\tau, \tau)$ verify the PE condition (7) under the adequate matrix of basis functions.

V. Physics Informed Extensions

In the previous section we deal with the trajectory inference problem using only states measurements and knowledge of the nonlinear dynamic model structure. In those cases we parametrize the nonlinear model as a product of a regressor matrix composed of nonlinear terms and a vector of parameters. These formulations are too conservative due to the structure knowledge assumption. In this section, we vanish this structure assumption by constructing a physics informed recurrent neural network, which uses a matrix of parameters and a vector of basis functions composed of the nonlinear terms of the nonlinear model. This slightly modification allows the inference model to have a linear combination of the basis functions that enhance the trajectory inference precision. In addition, if we have access to the control input then we can design an identification algorithm to estimate accurately the parameters of the nonlinear model.

A. Physics Informed Recurrent Neural Network

Notice that the proposed physics informed formulation can be regarded as a continuous-time parallel recurrent neural network (RNN) without hidden layers [45]. That is, the nonlinear function can be expressed as

$$\dot{x}_\tau = W^\top \Phi_w(x_\tau, u_\tau) \tag{42}$$

where $W \in \mathbb{R}^{p_w \times n}$ is a matrix of parameters or weights, and $\Phi_w(x,u) : \mathbb{R}^n \times \mathbb{R}^m \to \mathbb{R}^{p_w}$ is a vector of basis functions. Both (9) and (42) are equivalent and they differ in how the linear parameterization is constructed.

The PIM has the next structure

$$\dot{y} = \widehat{W}^\top \Phi_w(y, v), \tag{43}$$

where $\widehat{W} \in \mathbb{R}^{p_w \times n}$ is a matrix of parameter estimates of W. The state parameterizations of (42) and (43) are given by

$$\begin{aligned} x_\tau(t) &= e^{-\Lambda(t-t_0)} x_\tau(t_0) + W^\top h_w(x_\tau) + \Lambda l(x_\tau), \\ y(t) &= e^{-\Lambda(t-t_0)} x_\tau(t_0) + \widehat{W}^\top h_w(y) + \Lambda l(y), \end{aligned} \tag{44}$$

where $h_w(y) \in \mathbb{R}^{p_w}$ can be easily computed as

$$\dot{h}_w(y) = -\lambda h_w(y) + \Phi_w(y, v). \tag{45}$$

The identification error between the parameterizations in (44) is

$$\begin{aligned} e &= W^\top h_w(x_\tau) + \Lambda l(x_\tau) - \widehat{W}^\top h_w(y) + \Lambda l(y) \\ &= -\widetilde{W}^\top h_w(y) + \varepsilon_w, \end{aligned} \tag{46}$$

where $\widetilde{W} = \widehat{W} - W \in \mathbb{R}^{p_w \times n}$ defines the parametric error matrix and $\varepsilon_w = W^\top [h_w(x_\tau) - h_w(y)] + \Lambda [l(x_\tau) - l(y)] \in \mathbb{R}^n$ is the approximation error. Theorem 1 holds if the weights are updated as

$$\dot{W} = \Gamma h_w(y) e^\top. \tag{47}$$

Notice that each weight of matrix W defines a linear combination of basis functions and thus, some weights are zero because there are basis functions that do not contribute in one or more dimensions. However, (47) estimates all $p_w \times n$ weights of the network since it is not possible to set some weights to zero without compromising the stability of the RNN. Fig. 5 shows the general diagram of the physics informed RNN.

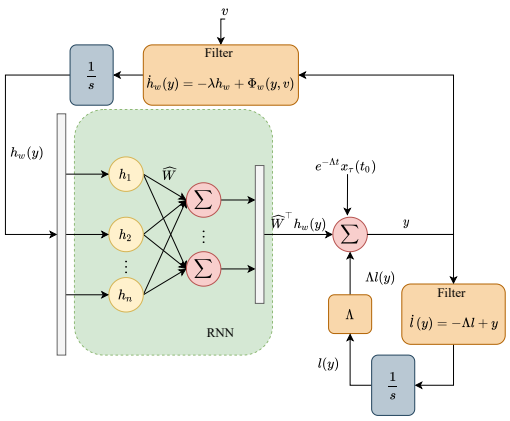

Fig. 5. Physics informed Recurrent Neural Network scheme

B. Identification of real parameter estimates

The previous approaches guarantee parameter estimates convergence under the fulfilment of a PE condition. However, the final estimates do not converge to their real values due to the addition of the PE signal in the states measurements output. In other words, if the PE signal is added directly to the output measurements then the amplitude of the PE signal increases or decreases the real parameter values; in consequence, the inference algorithm estimates different parameters that behaves similar to the real ones such that the output of the estimated model matches with the real system output.

To overcome this issue, and following standard identification algorithm techniques [46]–[48], we need to add the PE signal in the control input rather than in the output measurements. This implies, that we are enable to control the real system. In addition, by adding the PE signal in the real system's control input avoids the amplification/attenuation of the real parameter values.

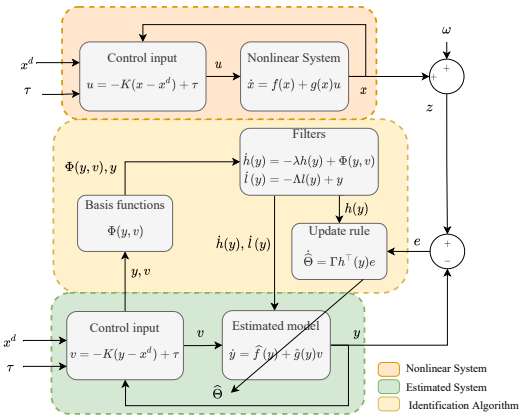

Fig. 6. Physics-Informed Diagram for Parameter Identification

For this case, we work with the nonlinear system (1) instead of (8). Then, the control input u and v have the next structure

$$\begin{aligned} u &= -K(z - x^d) + \tau, \\ v &= -K(y - x^d) + \tau. \end{aligned} \tag{48}$$

Notice that in contrast to previous approaches, we have access to the control input such that the controller is fed by the noisy states measurements.

Since we are able to control the real nonlinear system, then the desired trajectory is known in advance. So, the inference algorithm is reduced to an identification problem with filtering capabilities. Fig. 6 depicts the block diagram of the physics-informed algorithm for parameter identification purposes.

VI. Simulation studies

The effectiveness of the proposed approach is assessed in a F-16 aircraft model [49], [50]. The full roll-yaw dynamics of a F-16 aircraft in stability axis are

$$\begin{aligned}
\dot{\beta} =& \frac{Y_\beta}{V}\beta + \frac{Y_r}{V}r_s + \frac{g\cos\theta_0}{V}\phi - r_s,\\
\dot{\phi} =& \frac{\cos\gamma_0}{\cos\theta_0}p_s + \frac{\sin\gamma_0}{\cos\theta_0}r_s,\\
\dot{p}_s =& L_\beta\beta + L_p p_s + L_r r_s + L_{\delta_{a_0}}(\delta_a + f_1(\phi,\beta,p_s,r_s))\\
&+ L_{\delta_{r_0}}(\delta_r + f_2(\phi,\beta,p_s,r_s))\\
\dot{r}_s =& N_\beta\beta + N_p p_s + N_r r_s + N_{\delta_{a_0}}(\delta_a + f_1(\phi,\beta,p_s,r_s))\\
&+ N_{\delta_{r_0}}(\delta_r + f_2(\phi,\beta,p_s,r_s)),
\end{aligned}$$

where ϕ, β, p_s and r_s represent the roll angle, the sideslip, and the stability axis roll and yaw rates, respectively; θ_0 denotes the trimmed pitch angle, γ_0 is the trimmed flight path angle, V is the true airspeed, g is the gravitational constant, and δ_a, δ_r are aileron and rudder control. The functions $f_1(\cdot)$ and $f_2(\cdot)$ represent nonlinear functions in terms of the roll angle, the sideslip, and the stability axis roll and yaw rates. In these experiments, a lateral/directional F-16 model flying at sea level with an airspeed of 502 ft/s and an angle of attack $\alpha = 2.11^\circ$ is used. The model can be written compactly as the following nonlinear system

$$\dot{x} = Ax + Bu + f(x) + g(x)u,$$

where

$$A = \begin{bmatrix} -0.322 & 0.064 & 0.0364 & -0.9917\\ 0 & 0 & 1 & 0.0393\\ -30.6490 & 0 & -3.6784 & 0.6646\\ 8.5395 & 0 & -0.0254 & -0.4764 \end{bmatrix},$$

$$B = \begin{bmatrix} 0 & 0\\ 0 & 0\\ -0.7331 & 0.1315\\ -0.0319 & -0.062 \end{bmatrix}, \quad x = \begin{bmatrix} \beta\\ \phi\\ p_s\\ r_s \end{bmatrix}, \quad u = \begin{bmatrix} \delta_a\\ \delta_r \end{bmatrix},$$

$$f(x) = \begin{bmatrix} 0\\ 0\\ 0.7e^{-\frac{x_1^2}{2\cdot 1.5^2}} + 0.075\cos(0.1x_3 - 1.5)\sin(0.1x_4)\\ 0.7e^{-\frac{x_1^2}{2\cdot 1.5^2}} + 0.01\cos(0.1x_3 - 1.5)\sin(0.1x_4) \end{bmatrix}$$

$$g(x) = \begin{bmatrix} 0 & 0\\ 0 & 0\\ 0.7e^{-\frac{x_1^2}{2\cdot 1.5^2}} & 0\\ 0 & 0.7e^{-\frac{x_1^2}{2\cdot 1.5^2}} \end{bmatrix}.$$

Gaussian noise with mean zero and covariance $R = 0.1I$ is added at the output measurements to model sensor noise. The desired trajectory for the roll state ϕ^d is given by a square waveform trajectory of amplitude 1 and frequency 0.1 Hz, the desired trajectory of the other states are set to zero, that is, $[\beta^d, p_s^d, r_s^d] = [0, 0, 0]$ and hence $x^d = [\beta^d, \phi^d, p_s^d, r_s^d]^\top$. In addition, the low-pass filter $G(s) = \frac{30}{s+30}$ is used to smooth the roll trajectory.

Assume that the F-16 aircraft dynamics is controlled by a liner quadratic regulator (LQR) [6] using the next control gain

$$K = \begin{bmatrix} 36.0977 & -98.2690 & -94.5559 & -20.8372\\ 2.2735 & 19.2498 & 19.1944 & -91.8249 \end{bmatrix}.$$

Five cases of the physics-informed inference algorithm will be considered: Case A: Known control gain and trajectory, Case B: Unknown control gain and known trajectory, Case C: Unknown control gain and trajectory, Case D: Parallel Recurrent Neural Network, and Case E: System Identification. The number of parameters for each case are different but straightforward to determine since the structure of the nonlinear model is known in advance. For Cases A,B,C and E, the number of parameters is equal to the number of different non-zero coefficients associated to each basis functions. For Case D, the number of parameters is equal to the number of different basis functions times the number of dimensions of the nonlinear system. So, the number of parameters for case A: $\Theta \in \mathbb{R}^{22}$, case B: $\Xi \in \mathbb{R}^{26}$, case C: $\Omega \in \mathbb{R}^{26}$, case D: $W \in \mathbb{R}^{12\times 4}$, and case E: $\Theta \in \mathbb{R}^{22}$. In consequence the regressor matrices have the following dimensions $\Phi \in \mathbb{R}^{22\times 4}$, $\Psi \in \mathbb{R}^{26\times 4}$, $\Omega \in \mathbb{R}^{26\times 4}$, $\Phi_w \in \mathbb{R}^{12}$, and $\Phi \in \mathbb{R}^{22\times 4}$.

The PE signal τ is designed as an exponential sinusoidal function with different frequencies. On the other hand, the PE condition (7) cannot be established in practice because they need to verify the positive definiteness of the integral of the product of basis functions in a time window $[t : t + T]$ for all time t. To overcome this issue, consider the next weighted scalar PE condition

$$\beta_{w_1} \leq \int_t^{t+T} w^\top \Pi(s)\Pi^\top(s) w ds \leq \beta_{w_2}, \tag{49}$$

where $\Pi(\cdot) \in \mathbb{R}^{p_\pi \times n}$ is any matrix or vector (for case D) of basis functions with p_π parameters, $w = \frac{1}{\sqrt{p_\pi}}\vec{1}_{p_\pi}$ is a weight vector, $\vec{1}_{p_\pi} = \begin{bmatrix} 1 & \cdots & 1 \end{bmatrix}^\top \in \mathbb{R}^{p_\pi}$, and $\beta_{w_1}, \beta_{w_2}, T > 0$. Fig. 7 exhibits the fulfilment of the weighted PE condition in a time $t = 50$ s and $T = 5$s.

Note that in addition to verifying the weighted PE condition (49), some peculiarities can also be observed. For cases B and C we need to estimate more parameters in comparison to case A which translates into a weighted sum of quadratic excitation signals τ. This fact can be clearly observed in the amplitude of the weighted PE condition. Similar results can be observed for case D because the number of basis functions of the RNN increases n times. On the other hand, case E exhibits a clear attenuation of the PE amplitude since the excitation signal τ is not affected by the control gain K as it is stated in the control input v in (48).

The gain Γ of the update rule and Λ of the low pass filter are manually tuned until the best performance of the

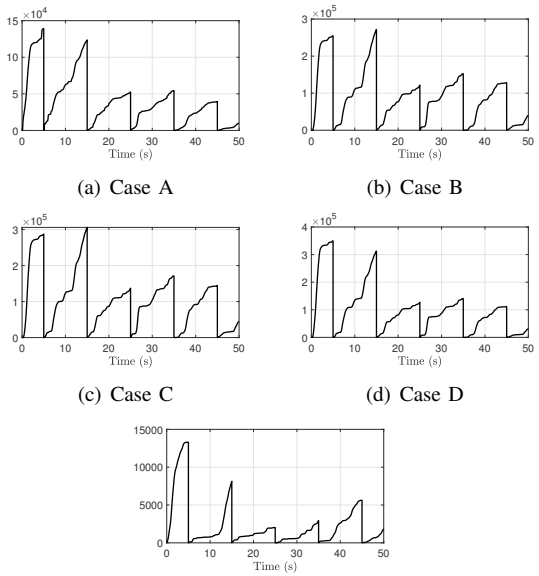

(a) Case A (b) Case B

(c) Case C (d) Case D

(e) Case E

Fig. 7. Weighted scalar PE condition results

TABLE I
GAINS FOR THE UPDATE RULE AND LOW-PASS FILTER

Case	Gains	
	λ	Γ
A	500	$2000I_{22}$
B	20	$500I_{26}$
C	20	$500I_{26}$
D	500	$2000I_{12}$
E	500	diag{500, 500, 500, 500, 500, 500, 50000, 500, 5000, 5000, 500, 500, 500, 500, 500, 500, 500, 500, 500, 500, 500, 500}

algorithm is achieved. However, a strong relation between the gain Γ, Λ and the excitation signal τ is observed. The filter's gain λ must be selected large enough such that the high frequencies of the excitation signal τ are not attenuated to guarantee parameter convergence. However, large gains λ and Γ can cause oscillations at the estimated states. Conversely, small values for Γ and λ causes parameter estimates drifting and state estimates with high variance and bias. The final gain values for each case are summarized on Table I.

The trajectory inference and parameter estimates convergence of each case are exhibited in Fig. 8. The figures show an accurate trajectory inference with noise attenuation for either known and unknown references. On the other hand, convergence of the parameter estimates is achieved in all cases. However, cases A, B, C, and D do not converge to their real values. Notice that for cases B and C the magnitude of the estimates is bigger because the values of the control gain K are incorporated in the estimates $\widehat{\Xi}$ and $\widehat{\Sigma}$, respectively. Case D exhibits good trajectory inference with good noise attenuation; furthermore, the weights of the net converge and remain bounded. The parameter estimates of case E converge to almost their real values and noise attenuation is exhibited in the output of the estimated model y. The approximation error results $\|\varepsilon\|$ are Case A: 0.0755, Case B: 0.107, Case C: 0.153, Case D: 0.0707, and Case E: 0.0477. The results highlight the consistence of the proposed methodology, that is, the more we know about the nonlinear system structure, input, and states then the approximation error will be small. Conversely, the less we know implies that the approximation error will be large. The RNN case demonstrates that if the number of basis functions are increased, then we are able to obtain a better approximation and robustness against modelling uncertainty. Furthermore, if the PE signal is added at the control input rather than the output measurements, then the approximation error is notably decreased.

Table II presents the final estimates values of case E and their respective parametric error percentage. Since the states measurements x of the real system are corrupted with noise, then the parameter estimates are UUB as it is stated in Theorem 1 and hence, the parameter estimates converge to their near real values.

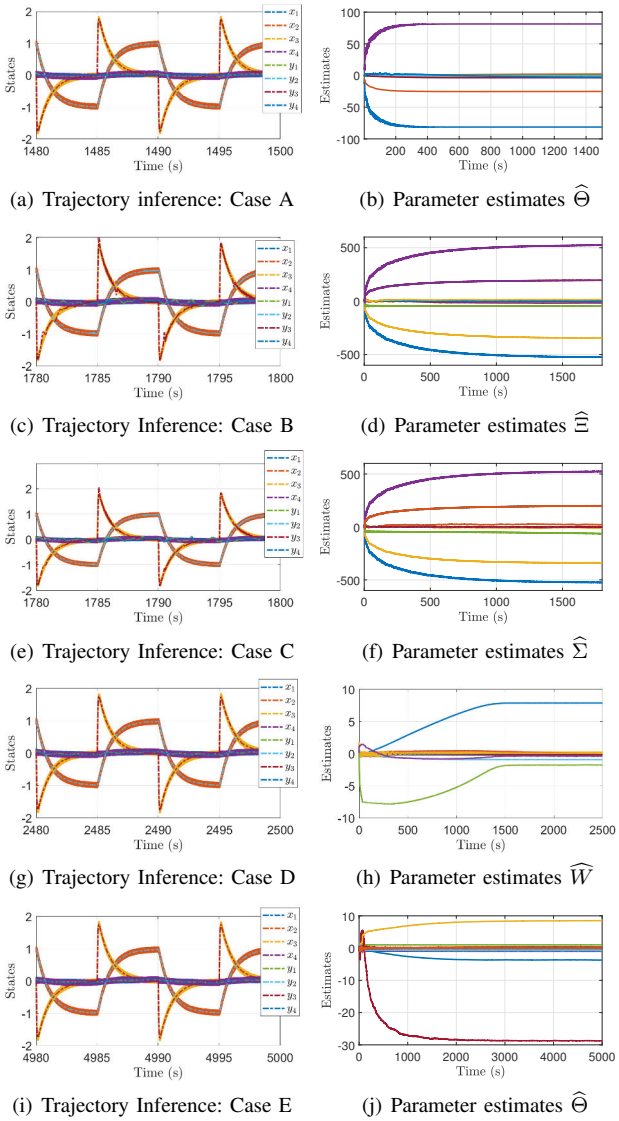

(a) Trajectory inference: Case A (b) Parameter estimates $\widehat{\Theta}$

(c) Trajectory Inference: Case B (d) Parameter estimates $\widehat{\Xi}$

(e) Trajectory Inference: Case C (f) Parameter estimates $\widehat{\Sigma}$

(g) Trajectory Inference: Case D (h) Parameter estimates $\widehat{W}$

(i) Trajectory Inference: Case E (j) Parameter estimates $\widehat{\Theta}$

Fig. 8. Physics-informed results

The norms of the identification error $\|e\|$ and the approximation error $\|\varepsilon\|$ are computed to verify the theoretical bounds of Theorem 1. The upper-bound $\beta_{w_2} = 13,800$ and lower bound $\beta_{w_1} = 2,000$ are obtained from the complete weighted PE

TABLE II
PARAMETER IDENTIFICATION RESULTS

Real parameter value Θ_i	Estimate value $\widehat{\Theta}_i$	Parametric error $\widetilde{\Theta}_i$	Percentage error $\lvert\widetilde{\Theta}_i\rvert$ (%)
-0.322	-0.3324	0.0104	3.2303
0.064	0.0652	-0.0012	1.8838
0.0364	0.0362	0.0002	0.5229
-0.9917	-1.0147	0.0230	2.3175
1	0.9997	0.0003	0.0295
0.0393	0.0391	0.0002	0.455
-30.649	-28.7241	-1.9249	6.2805
-3.6784	-3.6743	-0.0041	0.1107
0.6646	0.4432	0.2214	33.3158
8.5395	8.4799	0.0596	0.6984
-0.0254	-0.0193	-0.0061	23.8192
-0.4764	-0.6825	0.2061	43.252
-0.7331	-0.7365	0.0034	0.4635
0.1315	0.1153	0.0162	12.3504
-0.0319	-0.0318	-0.0001	0.4651
-0.062	-0.0607	-0.0013	2.1263
0.7	0.689	-0.011	1.5714
0.075	0.072	-0.003	4
0.7	0.688	-0.012	1.7143
0.01	0.0091	-0.0009	9
0.7	0.691	-0.009	1.2857
0.7	0.685	- 0.015	2.1429

plot of Fig. 7(e). We need to scale the parametric error by the number of parameters p_π to recover the effect of the real bounds of the initial PE condition (7). Consider $N = 1$ time-windows and $p_\pi = 22$. The numerical results are: $\|e\| = 0.1$, $\|\varepsilon\| = 0.0477$, $\|\widetilde{\Theta}\| = 1.95$. The above results are consistent to the theoretical upper bounds (21) and (20), that is, $\|e\| \leq (\frac{\beta_{w_2}}{\beta_{w_1}} + 1)\bar{\varepsilon} \approx 0.3713$ and $\|\widetilde{\Theta}\| \leq \frac{2\lambda}{\beta_{w_1} N}\sqrt{\frac{\beta_{w_2} N}{2\lambda}}\bar{\varepsilon}p_\pi \approx 1.9206$. If we consider more time-windows N this inequality is more strict and difficult to guarantee if the excitation signal τ is not rich enough.

A. Comparisons and Robustness

An extended Kalman Filter (EKF) is used to exhibit the sensitivity of state estimators under model uncertainty. Notice that data-driven methods cannot be used for a fair comparison study since most of them are off-line, whilst the proposed approach is on-line. On the other hand, other on-line approaches such as Gaussian processes need access to the control input using mechanisms inspired in reinforcement learning architectures, e.g., exploration strategies.

Two different scenarios are used to test the EKF: 1) an approximate nonlinear model without control input measurements, and 2) an approximate nonlinear model with control input measurements. The results are shown in Fig. 9. Some

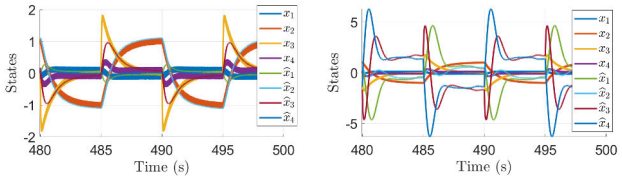

(a) Without control measurements (b) With control measurements

Fig. 9. State estimation results using Extended Kalman filter

interesting results are obtained; the first evident result is that the EKF without control measurements (EKF_{wc}) exhibits better results than the EKF with control (EKF_c). Here, the modelling error associated to the input dynamics affects the accuracy of the estimates. However, the model without control suffers of adaptability to new references. On the other hand, the EKF with control gives a notion of the hidden reference which can be useful for adaptation to new references. However, it lacks of accuracy in the estimates due to the modelling error.

The estimation error for both approaches are $\|e_{EKF_{wc}}\| = 0.2439$ and $\|e_{EKF_c}\| = 3.401$. Recall that the estimation error of the proposed approach is $\|e\| = 0.1$ for Case E. Here, we can observe the reliability and robustness of the proposed approach in comparison to the EKF results. The merits of the approach can be summarized as follows: i) accurate trajectory inference is obtained without any prior knowledge of the system's parameters, ii) the complete set of basis functions give stability to the approach without applying any linearization or data-driven methods, and iii) the robustness of the approach depends on the set of basis functions which can incorporate different non-linear functions that are capable to compensate model uncertainty and disturbances.

VII. CONCLUSIONS

This work reports a physics informed trajectory inference algorithm for a class of nonlinear systems. It combines the advantages of state and parameter estimation algorithms in one simple architecture based on the construction of an estimated model and the design of two low-pass filters. The algorithm exhibits an equivalence to parallel recurrent neural networks and can be expanded for different cases depending of the available information of the control gain, the desired trajectory, and the set of basis functions. In addition, the approach can be used for pure identification purposes. Stability and convergence of the inference algorithm is assessed using Lyapunov stability theory. Simulation studies are carried out to verify the effectiveness of the approach under different scenarios. The results show that the algorithm infers the trajectory with high accuracy and noise attenuation. Furthermore, the parameter estimates converge and are UUB. For identification purposes, the parameter estimates have good precision results which can be improved by modifying the gains of the update rule.

Further work focuses on the design of a self-learning model for non-parametric basis functions inference and time-varying parameters. Furthermore, the design of PE signals is still an open challenge which is crucial for parameter estimates convergence in finite time.

REFERENCES

[1] C. M. Legaard, T. Schranz, G. Schweiger, J. Drgoňa, B. Falay, C. Gomes, A. Iosifidis, M. Abkar, and P. G. Larsen, "Constructing neural network-based models for simulating dynamical systems," *arXiv preprint arXiv:2111.01495*, 2021.

[2] W. Gilpin, "Chaos as an interpretable benchmark for forecasting and data-driven modelling," *arXiv preprint arXiv:2110.05266*, 2021.

[3] E. Archer, I. M. Park, L. Buesing, J. Cunningham, and L. Paninski, "Black box variational inference for state space models," *arXiv preprint arXiv:1511.07367*, 2015.

[4] R. Rezaie and X. R. Li, "Destination-directed trajectory modeling, filtering, and prediction using conditionally markov sequences," *IEEE Transactions on Aerospace and Electronic Systems*, vol. 57, no. 2, pp. 820–833, 2020.

[5] X. Li, G. Fan, K. Pan, G. Wei, C. Zhu, G. Rizzoni, and M. Canova, "A physics-based fractional order model and state of energy estimation for lithium ion batteries. part i: Model development and observability analysis," *Journal of Power Sources*, vol. 367, pp. 187–201, 2017.

[6] B. Kiumarsi, K. G. Vamvoudakis, H. Modares, and F. L. Lewis, "Optimal and autonomous control using reinforcement learning: a survey," *IEEE Transactions on Neural Networks and Learning Systems*, vol. 29, no. 6, pp. 2042–2062, 2018.

[7] A. Perrusquía and W. Yu, "Neural $\mathcal{H}_2$ control using continuous-time reinforcement learning," *IEEE Transactions on Cybernetics*, vol. 52, no. 6, pp. 4485–4494, 2022.

[8] W. Yu and A. Perrusquía, "Simplified stable admittance control using end-effector orientations," *International Journal of Social Robotics*, vol. 12, no. 5, pp. 1061–1073, 2020.

[9] Z. Peng, Y. Jiang, L. Liu, and Y. Shi, "Path-guided model-free flocking control of unmanned surface vehicles based on concurrent learning extended state observers," *IEEE Transactions on Systems, Man, an Cybernetics: Systems*, 2023.

[10] X. Zheng, M. Zaheer, A. Ahmed, Y. Wang, E. P. Xing, and A. J. Smola, "State space lstm models with particle mcmc inference," *arXiv preprint arXiv:1711.11179*, 2017.

[11] P. Becker, H. Pandya, G. Gebhardt, C. Zhao, C. J. Taylor, and G. Neumann, "Recurrent kalman networks: Factorized inference in high-dimensional deep feature spaces," in *International Conference on Machine Learning*. PMLR, 2019, pp. 544–552.

[12] R. Corteso, J. Park, and O. Khatib, "Real-time adaptive control for haptic telemanipulation with kalman active observers," *IEEE Transactions on Robotics*, vol. 22, no. 5, pp. 987–999, 2006.

[13] C. Wang, H. Han, J. Wang, H. Yu, and D. Yang, "A robust extended kalman filter applied to ultrawideband positioning," *Mathematical Problems in Engineering*, vol. 2020, 2020.

[14] L. B. White and F. Carravetta, "State-space realizations and optimal smoothing for gaussian generalized reciprocal processes," *IEEE Transactions on Automatic Control*, vol. 65, no. 1, pp. 389–396, 2019.

[15] R. Rezaie and X. R. Li, "Gaussian conditionally markov sequences: Modeling and characterization," *Automatica*, vol. 131, p. 109780, 2021.

[16] P. Geragersian, I. Petrunin, W. Guo, and R. Grech, "An ins/gnss fusion architecture in gnss denied environment using gated recurrent unit," in *AIAA SCITECH 2022 Forum*, 2022, p. 1759.

[17] T. Raïssi and M. Aoun, "On robust pseudo state estimation of fractional order systems," in *International Symposium on Positive Systems*. Springer, 2016, pp. 97–111.

[18] A. Azami, S. V. Naghavi, R. Dadkhah Tehrani, M. H. Khooban, and F. Shabaninia, "State estimation strategy for fractional order systems with noises and multiple time delayed measurements," *IET Science, Measurement & Technology*, vol. 11, no. 1, pp. 9–17, 2017.

[19] R. G. Brown and P. Y. Hwang, "Introduction to random signals and applied kalman filtering: with matlab exercises and solutions," *Introduction to random signals and applied Kalman filtering: with MATLAB exercises and solutions*, 1997.

[20] L. Xu and R. Niu, "Ekfnet: Learning system noise statistics from measurement data," in *ICASSP 2021-2021 IEEE International Conference on Acoustics, Speech and Signal Processing (ICASSP)*. IEEE, 2021, pp. 4560–4564.

[21] A. Perrusquía and W. Guo, "Closed-loop output error approaches for drone's physics informed trajectory inference," *IEEE Transactions on Automatic Control*, 2023.

[22] O. Nelles, "Nonlinear dynamic system identification," in *Nonlinear System Identification*. Springer, 2020, pp. 831–891.

[23] D. Li, B. Zhang, P. Li, E. Q. Wu, R. Law, X. Xu, A. Song, and L.-M. Zhu, "Parameter estimation and anti-sideslip line-of-sight method-based adaptive path-following controller for a multijoint snake robot," *IEEE Transactions on Systems, Man, and Cybernetics: Systems*, 2023.

[24] T. Yamammoto, M. Bernhardt, A. Peer, M. Buss, and A. M. Okammura, "Techniques for Environment parameter Estimation during telemanipulation," *Proceedings of the 2nd Biennial IEEE/RAS-EMBS International Conference on Biomedical Robotics and Biomechatronics*, 2008.

[25] A. Perrusquía and W. Guo, "A closed-loop output error approach for physics-informed trajectory inference using online data," *IEEE Transactions on Cybernetics*, vol. 53, pp. 1379–1391, 2023.

[26] I. D. Landau and A. Karimi, "An output error recursive algorithm for unbiased identification in closed loop," *Automatica*, vol. 33, no. 5, 1997.

[27] A. Janot, P.-O. Vandanjon, and M. Gautier, "A generic instrumental variable approach for industrial robot identification," *IEEE Transactions on Control Systems Technology*, vol. 22, no. 1, pp. 132–145, 2013.

[28] A. Perrusquía, "Robust state/output feedback linearization of direct drive robot manipulators: A controllability and observability analysis," *European Journal of Control*, 2022.

[29] S. Zeng and E. Fernandez, "Adaptive controller design and disturbance attenuation for sequantially interconnected SISO linear systems under noisy output measurements with partly measured disturbances," *2008 American Control Conference*, 2008.

[30] R. Garrido and R. Miranda, "DC servomechanism parameter identification: A closed loop input error approach," *ISA Transactions*, vol. 51, pp. 42–49, 2012.

[31] A. Perrusquía, R. Garrido, and W. Yu, "Stable robot manipulator parameter identification: A closed-loop input error approach," *Automatica*, vol. 141, p. 110294, 2022.

[32] M. Brunot, A. Janot, F. Carrillo, J. Cheong, and J.-P. Noël, "Output error methods for robot identification," *Journal of Dynamic Systems, Measurement, and Control*, vol. 142, no. 3, 2020.

[33] I. D. Landau and A. Karimi, "An output error recursive algorithm for unbiased identification in closed loop," *Automatica*, vol. 33, no. 5, pp. 933–938, 1997.

[34] C. Urrea and J. Pascal, "Design and validation of a dynamic parameter identification model for industrial manipulator robots," *Archive of Applied Mechanics*, pp. 1–27, 2021.

[35] M. Gautier, A. Janot, and P.-O. Vandanjon, "A new closed-loop output error method for parameter identification of robot dynamics," *IEEE Transactions on Control Systems Technology*, vol. 21, no. 2, 2013.

[36] M. Brunot, A. Janot, P. C. Young, and F. Carrillo, "An improved instrumental variable method for industrial robot model identification," *Control Engineering Practice*, vol. 74, pp. 107–117, 2018.

[37] A. Janot, M. Gautier, A. Jubien, and P. O. Vandanjon, "Comparison between the cloe method and the didim method for robots identification," *IEEE Transactions on Control Systems Technology*, vol. 22, no. 5, pp. 1935–1941, 2014.

[38] A. Perrusquía, R. Garrido, and W. Yu, "An input error method for parameter identification of a class of euler-lagrange systems," in *2021 18th International Conference on Electrical Engineering, Computing Science and Automatic Control (CCE)*. IEEE, 2021, pp. 1–6.

[39] F. L. Lewis, D. Vrabie, and K. G. Vamvoudakis, "Reinforcement learning and feedback control using natural decision methods to design optimal adaptive controllers," *IEEE Conrol Systems Magazine*, vol. 32, no. 6, pp. 76–105, 2012.

[40] K. G. Vamvoudakis, "Q-learning for continuous-time linear systems: A model-free infinite horizon optimal control approach," *Systems & Control Letters*, pp. 14–20, 2017.

[41] K. Vamvoudakis and F. L. Lewis, "On-line actor-critic algorithm to solve the continuous-time infinite horizon optimal control problem," *Automatica*, vol. 46, pp. 878–888, 2010.

[42] F. Lewis, S. Jagannathan, and A. Yeşildirek, *Neural Network control of robot manipulators and nonlinear systems*. Taylor & Francis, 1999.

[43] S. A. A. Rizvi and Z. Lin, "Output feedback q-learning control for the discrete-time linear quadratic regulator problem," *IEEE transactions on neural networks and learning systems*, vol. 30, no. 5, pp. 1523–1536, 2018.

[44] A. Perrusquía, "Solution of the linear quadratic regulator problem of black box linear systems using reinforcement learning," *Information Sciences*, vol. 595, pp. 364–377, 2022.

[45] A. Perrusquía and W. Yu, "Identification and optimal control of nonlinear systems using recurrent neural networks and reinforcement learning: An overview," *Neurocomputing*, vol. 438, pp. 145–154, 2021.

[46] A. Janot, M. Gautier, A. Jubien, and P. O. Vandanjon, "Comparison between the CLOE method and the DIDIM method for robot identification," *IEEE Transactions on Control Systems Technology*, vol. 22, no. 5, 2014.

[47] S. Briot and M. Gautier, "Global identification of joint drive gains and dynamic parameters of parallel robots," *Multibody System Dynamics*, vol. 33, no. 1, pp. 3–26, 2015.

[48] D. Jung, J. Cheong, D. Park, and C. Park, "Backward sequential approach for dynamic parameter identification of robot manipulators," *International Journal of Advanced Robotic Systems*, vol. 15, no. 1, pp. 1–10, 2018.

[49] A. Young, C. Cao, N. Hovakimyan, and E. Lavretsky, "An adaptive approach to nonaffine control design for aircraft applications," in *AIAA guidance, navigation, and control conference and exhibit*, 2006, p. 6343.

[50] H. Vo and S. Seshagiri, "Robust control of f-16 lateral dynamics," in *2008 34th annual conference of IEEE industrial electronics*. IEEE, 2008, pp. 343–348.

2023-08-10

Physics informed trajectory inference of a class of nonlinear systems using a closed-loop output error technique

Perrusquía, Adolfo

IEEE

Perrusquia A, Guo W. (2023) Physics informed trajectory inference of a class of nonlinear systems using a closed-loop output error technique. IEEE Transactions on Systems, Man, and Cybernetics: Systems, Volume 53, Issue 12, December 2023, pp. 7583-7594
https://doi.org/10.1109/TSMC.2023.3298217